Unusual anatomy of the ectoparasitic muricid *Vitularia salebrosa* (King and Broderip, 1832) (Neogastropoda: Muricidae) from the Pacific coast of Panama

Luiz Ricardo L. Simone
Museu de Zoologia da Universidade de São Paulo
C.P. 42494
04299-970 São Paulo, BRAZIL
lrsimone@usp.br

Gregory S. Herbert
Department of Geology
University of South Florida
4202 East Fowler Avenue
Tampa, FL 33620 USA
gherbert@cas.usf.edu

Didier Merle
Département Histoire de la Terre (CP 38)
UMR 5143 & USM 203
Paléobiodiversité et Paléoenvironnements
Muséum National d'Histoire Naturelle
8, rue Buffon
F-75005 Paris, FRANCE
dmerle@mnhn.fr

ABSTRACT

The morphology and anatomy of *Vitularia salebrosa*, a muricid ectoparasitic on other mollusks, are investigated based on study of specimens from western Panama. Distinctive characters of this species include the small size of the buccal mass and radular apparatus, simplification of the odontophore muscles and diminished lateral teeth of the radula; an elongated, narrow proboscis; narrow digestive tract and a differentiable glandular region at the beginning of the posterior esophagus. These traits are consistent with adaptive specialization for an ectoparasitic life history.

INTRODUCTION

Herbert et al. (2009) have shown that *Vitularia salebrosa* (King and Broderip, 1832) is an ectoparasitic gastropod that can feed suctorially on a single molluscan host for months by drilling through the host's hell and inserting its proboscis into the host's blood supplies and organs. One of the questions raised in that study was whether and to what degree the anatomy of *V. salebrosa* has undergone adaptive specialization for an ectoparasitic lifestyle. For example, foot scars formed by *V. salebrosa* on the surface of its host's shell suggest that this ectoparasite produces mucous adhesives in its foot to help it attach itself securely to prey during feeding (Herbert et al., 2009). D'Attilio (1991) and Herbert et al. (2008) also reported the absence of a radula in 80–90% of *V. salebrosa* individuals examined. Radula loss is characteristic of the muricid subfamily Coralliophilinae, which are highly specialized ectoparasites of cnidarians.

The objective of this study is to describe for the first time the anatomy of *Vitularia salebrosa* to serve as basis for further comparisons with other muricids and contribute to a systematic revision of the genus *Vitularia* Swainson, 1840 (type species: *Vitularia miliaris* (Gmelin, 1791)).

MATERIALS AND METHODS

Specimens were observed living, followed by dissections performed on specimens immersed in 70% ethanol and observed using a stereomicroscope. Scanning electron microscopy (SEM) was used to examine the radulae in the laboratory of Electron Microscopy of the Museu de Zoologia da Universidade de São Paulo. Drawings were made with the aid of a camera lucida, and dissections were also digitally photographed. The conchological description uses the terminology of Merle (2001, 2005). Acronyms for collections cited in this paper are **MZSP**, Museu de Zoologia da Universidade de São Paulo, and **PRI**, Paleontological Research Institution, Ithaca, New York, USA.

RESULTS

DESCRIPTION

Vitularia salebrosa (King and Broderip, 1832)
(Figures 1–33)

Murex salebrosus King and Broderip, 1832: 347.
Vitularia salebrosa: Keen, 1971: 536 (fig. 1040); Radwin and D'Attilio, 1976: 173–174 (figs. 114, 115; pl. 7, fig. 14); Ramírez et al., 2003: 261; Paredes et al., 2004: 214.

Shell (Figures 1–3, 6–8): Shell surface pustulose. Protoconch multispiral, with numerous granules, aligned in axial and spiral directions. Sinusigeral scar well marked. Early teleoconch whorl with P1 cord. Axial sculpture with lamellose varices. Adult teleoconch with only P1 evident. Infrasutural denticle split, eight internal denticles present, perhaps corresponding to D1 to D6 or D1 to D5 (with several split denticles). Columellar

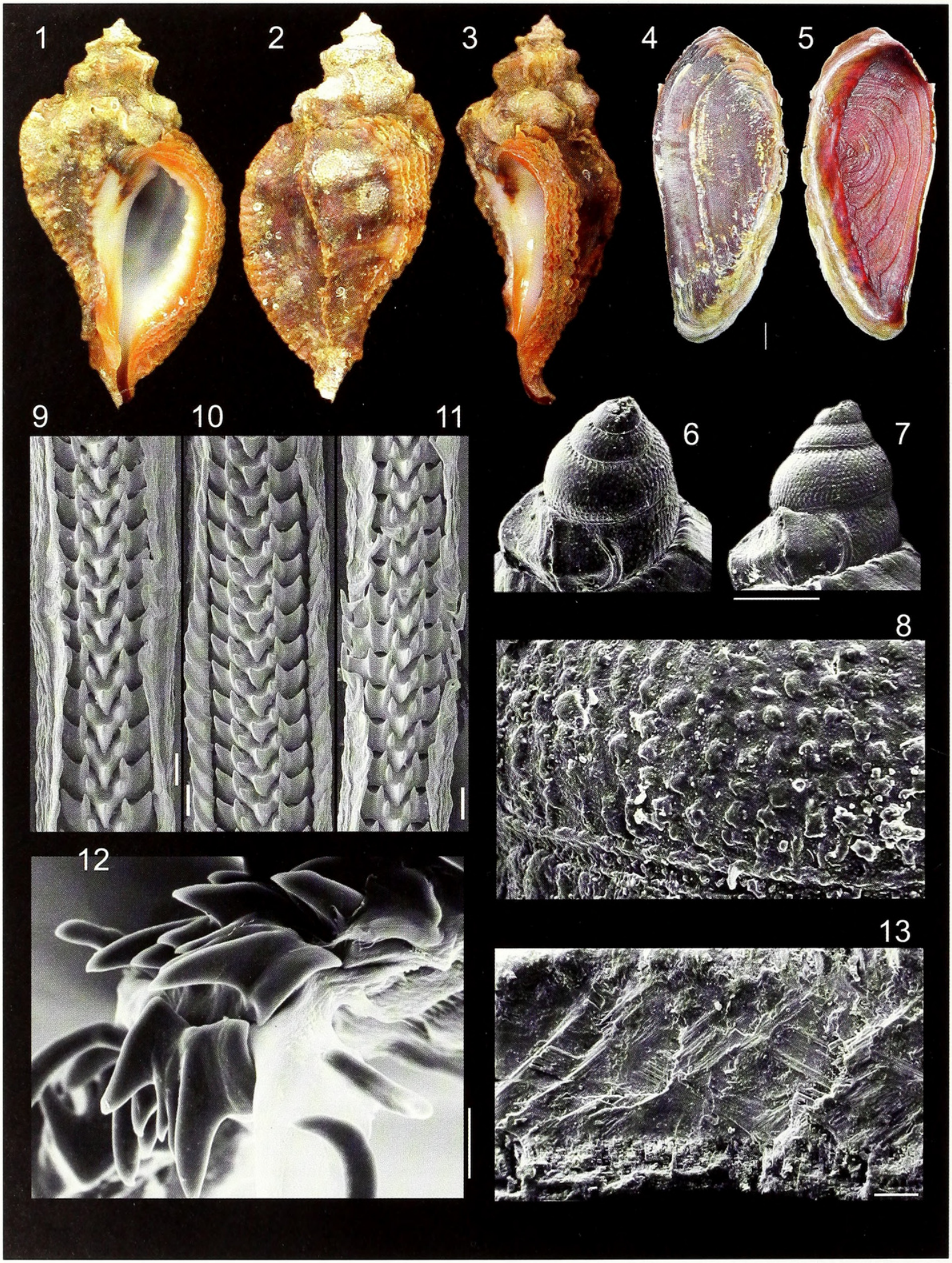
1
2
3
4
5
9
10
11
6
7
8
12
13

tubercles absent. Microstructure with three shell layers; an innermost, thin aragonite layer, a thick, middle aragonite layer, and one thin, outer calcite layer (Figure 13). Complementary descriptions in Radwin and D'Attilio (1976: 173–174) and Herbert et al. (2009).

Head-Foot (Figures 14, 15, 20): Head not protruded, small (about 1/4 of adjacent width of head-foot). Tentacles stubby, broad, flat, broader basally; length about 1/3 of wider width of head-foot. Eyes dark, small, situated in middle region of outer edge of tentacles. Tentacles situated close to each other, with space between them about 1/2 the tentacular width. Rhynchostome a small, transverse slit located between and slightly ventral to tentacles. Foot large, spanning about 1/2 whorl. Anterior furrow of pedal glands exending along entire anterior edge of foot. Columellar muscle thick, about 3/4 whorl in length. Haemocoel long, slightly broader anteriorly and narrower posteriorly (Figure 20). Accessory boring organ (ABO) very narrow and relatively deep (about 1/4 of foot thickness), better developed and associated with cement gland in females (Figure 15, **fc**); sharing the same aperture.

Operculum (Figures 4, 5): Suboval, filling entire aperture. Superior edge rounded; inferior edge broadly pointed; inner edge almost straight in inferior half and rounded in superior half; outer edge uniformly rounded. Outer surface opaque, mostly smooth; conspicuous scales parallel to edge in superior and inferior slopes of outer edge. Nucleus at middle level of outer margin. Attachment scar occupying about 80% of inner surface, with concentric, somewhat uniform undulations. Outer margin glossy, uniform in width (about 1/4 opercular width) along entire length of operculum.

Mantle Cavity Organs (Figures 16, 18): Mantle cavity spans about one whorl. Mantle border simple, slightly thickened. Siphon comprises about 1/3 of free portion of mantle edge width and about 1/3 whorl in length. Right edge of siphon base forming tall fold that runs parallel to mantle edge and extends approximately 1/2 width of mantle cavity (Figure 16, se); middle region of this fold tall (about 1/2 of mantle cavity height), right end of this fold diminishing gradually, becoming weaker near mantle edge. Osphradium elliptical, 1/4 mantle cavity length, 1/5 of mantle cavity roof width. Osphradium leaflets very low (about 1/4 width); tips sharply pointed, turned externally. Anterior portion of osphradium well-separated from gill. Osphradial nerve enters in middle region of osphradial ganglion (Figure 16, **on**). Ctenidial vein (efferent branchial vessel) uniformly narrow, along its length. Ctenidial longitudinal muscle covers about 3/4 of ventral surface of ctenidial vein (Figure 18, **gm**). Ctenidium elongated, spanning 85% of mantle cavity length, about 1/2 its width. Anterior end of ctenidium pointed, inserted into right surface of tall fold formed by right siphonal base. Ctenidium uniform in width along most of its length, increasing in size relatively abruptly toward the posterior margin. Posterior end of ctenidium rounded, situated close to posterior end of mantle cavity and to pericardium. Ctenidial filaments triangular, spanning ~1/2 mantle cavity height, apex central, slightly turned to right, left and right edges straight. Afferent ctenidial vessel very narrow, running along right margin of gill. Space between ctenidium and right pallial organs roughly 1/2 gill width. Hypobranchial gland thin, with uniform surface, pale-beige, covering most of area between the gill and right pallial structures. Right side of mantle cavity nearly filled by gonoducts (Figures 16, 32). Rectum very narrow, almost filiform, running along right edge of mantle cavity in young specimens, dislocated to left by gonoducts of mature specimens. Anus very small, situated at 1/4 mantle cavity length from mantle edge, with small terminal papilla (Figures 16, 32, **ap**).

Visceral Mass (Figures 26, 29): Visceral mass tapering, spanning ~2½ whorls posterior to the mantle cavity. Digestive gland pale-beige with small black spots, occupying most of the visceral mass, surrounding the stomach, extending from visceral apex to kidney-pericardium. Gonad also pale-beige, situated along the columellar surface of the digestive gland, extending from the first whorl to 1/2 whorl posterior to stomach.

Circulatory and Excretory Systems (Figure 17): Reno-pericardial region spanning ~1/3 whorl, situated at anterior margin of visceral mass, partly adjacent to the mantle cavity, roughly triangular in cross-section, broadest along right margin. Pericardium occupying ~1/3 of reno-pericardial region, just posterior to gill at anterior-left margin of visceral mass (Figures 16, 29). Auricle anterior to ventricle, connected to ctenidial vein (efferent branchial vessel) at its left-anterior side, to reno-pericardial duct along its right side; distance between connections ~1/4 adjacent whorl width. Ventricle spherical, connected to aortas at its posterior-left side. Aortas narrow, anterior aorta about twice diameter of posterior aorta, running parallel to esophagus. Kidney somewhat elliptical in outline. Renal lobe single, mostly solid, with imbricated, septum-like, transverse, glandular folds, all connected at middle region of ventral surface by longitudinal efferent renal vessel coming from haemocoel; lobe surrounding intestine-rectum transition alongside right region; color cream, surface transversally folded, filling most of kidney inner space, not connected to ventral renal surface. Nephridial gland ~1/4 width of renal lobe, triangular in section; covering entire membrane between

Figures 1–13. *Vitularia salebrosa*, shells. **1–3.** PRI 9468, apertural, dorsal and profile views, length = 40.0 mm. **4–5.** Typical operculum, outer and inner views, scale bar = 2 mm. **6–8.** SEM of Protoconch, PRI 9469. **6.** Lateral-slightly apical view. **7.** Lateral view. **8.** Detail of sculpture of penultimate whorl, scale bar = 50 μm. **9–12.** Radulae of 3 specimens, SEM. Scale bars = 20 μm. **13.** Transverse section of shell, SEM, scale = 100 μm.

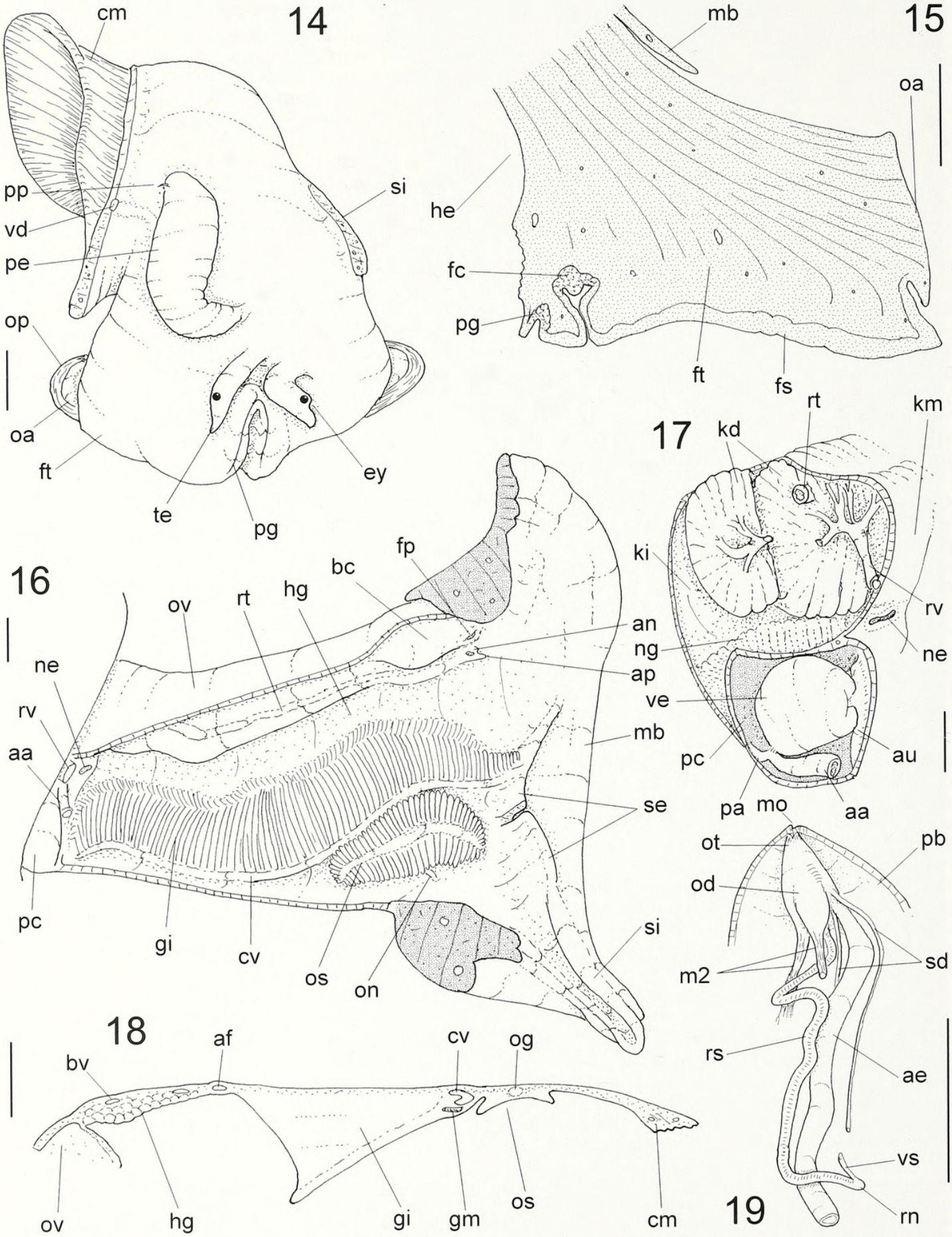
14
cm
pp
vd
pe
op
oa
ft
te
pg
si
ey
15
mb
oa
he
fc
pg
ft
fs
16
ov
rt
hg
bc
fp
ne
rv
aa
an
ng
ap
mb
se
pc
gi
cv
os
on
si
17
kd
rt
km
ki
rv
ne
ve
pc
au
pa
mo
aa
ot
pb
od
m2
sd
rs
ae
vs
rn
18
af
bv
cv
og
ov
hg
gi
gm
os
cm
19

kidney and pericardium, wider dorsally. Nephrostome a small slit in kidney wall in mantle cavity (Figures 16, 17, **ne**).

Digestive System (Figures 19–26): Proboscis narrow and very long (~3 times shell length, 1/4 haemocoel width), outer walls thin, muscular (Figures 20, 21). Pairs of ventral proboscis retractor muscles (**rm**) narrow, originating in dorsal surface of foot, concentrated along right region, just ventral to head (Figure 20); closer to buccal mass, retractor muscles almost imperceptible, embedded in proboscis wall (Figure 21). Mouth transverse, narrow. Oral tube short, broad, walls weakly muscular. Dorsal folds paired, originate along dorsal, inner surface of oral tube, become more longitudinal posteriorly (Figure 23, **df**), with a narrow, smooth surface between them. Odontophore very small, ~1/15 proboscis volume, situated just posterior to mouth (Figure 21, **od**). Odontophore and buccal mass muscles (Figures 23–25): **mj**, peribuccal muscles, paired, thick layers of muscles connected along both sides of anterior-outer margin of odontophore cartilages (Figures 24, 25), embedded in dorsal wall of buccal mass; **m1**, jugal muscles, several pairs of small, short fibers connecting buccal mass with adjacent inner surface of proboscis; **m2**, pair of retractor muscles of buccal mass (retractor of pharynx), originating in ventral surface of haemocoel (dorsal surface of foot sole) at mid-length, just posterior to proboscis retractor muscles, extend anteriorly and dorsally as a pair of inconspicuous longitudinal muscles, inserting into posterior end of both odontophore cartilages; **m4**, pair of large, broad, thin, dorsal tensor muscles of radula, originating along outer surface of cartilages, surrounding **mj** origin, covering most of cartilage surface (except edge close to median line), inserting mostly into subradular membrane, and also in a small region of tissue in radular ribbon (anterior to its exposed area) (Figures 24, 25, **to**); **m5**, pair of auxiliary dorsal tensor muscles of radula, thin, originating along median edges of cartilages along their posterior quarter, running medially and anteriorly, inserting along ventral portion of radular sac, crossing odontophore (opposite to **m4** insertions in tissues on radula); **m6**, horizontal muscle, relatively thin, connecting ventral edges of both cartilages, from anterior end of cartilages, posteriorly ~60% of their length; **m11**, paired ventral tensor muscles of radula, thin, narrow, originating at median-posterior ends of odontophore cartilages, extending dorsally to **m5** origins, running anteriorly at some distance from median line, inserting along anterior surface of ventral region of subradular membrane (Figure 24). Other non-muscular odontophore structures: **br**, subradular membrane, thin, semi-transparent, strong, connecting to **m4** muscle pair at lateral and anterior edges, covering inner surface of subradular cartilage; **sc**, subradular cartilage expansions, elliptical, covering about half of exposed portion of subradular membrane within buccal cavity, bearing exposed part of radula, expanding beyond it laterally equal to the width of the radula on each side; **oc**, odontophore cartilages, flat, long, paired, about 5 times as long as wide, elliptical in outline, anterior somewhat pointed, slightly wider than rounded posterior; **to**, tissue on radula posterior to its exposed portion within buccal cavity, located inside radular sac along its region crossing odontophore, **m4** muscle pair insert into it laterally along a region ~1/10 cartilage length. Radular sac narrow (~1/5 of odontophore width), long (4 times buccal mass length) (Figure 19). Radular nucleus (odontoblast region of radular sac) slightly broad, connected to inner surface of proboscis by relatively wide vessel with thin, muscular walls (Figure 19). Radular teeth (Figures 9–12): Rachidian teeth wide, ~3/5 of radular ribbon width, chevron-like, with 7 conical, pointed, posteriorly-directed cusps that are not aligned; central cusp taller, at a greater angle to ribbon than remaining, lateral cusps, which are situated nearly on the same plane; lateral edges of rachidian teeth broad, flattened. Lateral teeth paired, very narrow, ~1/8 of rachidian teeth width, equal to rachidian teeth in height (L/W ~5), weakly curved; bases wider, inserted into subradular cartilage close to proximal region of rachidian teeth lateral edge; tip sharply pointed, turned posteriorly. Salivary glands just posterior to valve of Leiblein, anterior to nerve ring (Figure 21, **sg**), occupying ~1/8 of haemocoel volume. Salivary gland ducts very narrow; gradually become embedded in anterior esophagus wall anterior to valve of Leiblein (Figure 21). Accessory salivary glands absent. Anterior esophagus narrow, long (Figure 21), equal in length to proboscis, inner surface smooth, with pair of low, narrow longitudinal folds in anterior region

Figures 14–19. *Vitularia salebrosa* anatomy. **14.** Head-foot, male, frontal view. **15.** Foot, female, longitudinal section in median line. **16.** Mantle cavity roof, female, ventral view, transversal section in fold of right base of siphon artificially done. **17.** Reno-pericardial region, ventral view, ventral wall of pericardium and part of kidney removed, posterior region of renal lobe partially deflected. **18.** Mantle cavity roof, female, transversal section in middle level of osphradium. **19.** Distal region of foregut, ventral-right view, distal portion of proboscis also shown. Scale bars = 2 mm. Abbreviations: **aa,** anterior aorta; **ae,** anterior esophagus; **af,** afferent branchial vessel; **an,** anus; **ap,** anal papilla; **au,** auricle; **bc,** bursa copulatrix; **bv,** blood vessel; **cm,** columellar muscle; **cv,** ctenidial vein; **ey,** eye; **fc,** female cement gland plus boring organ; **fp,** female pore; **fs,** foot sole; **ft,** foot; **gi,** gill; **gm,** gill longitudinal muscle; **he,** haemocoel; **hg,** hypobranchial gland; **kd,** kidney dorsal lobe; **ki,** kidney chamber; **km,** membrane between kidney and mantle cavity; **m2,** buccal mass and odontophore muscles; **mb,** mantle border; **mo,** mouth; **ng,** nephridial gland; **ne,** nephrostome; **oa,** opercular pad; **od,** odontophore; **og,** osphradium ganglion; **on,** osphradium nerve; **op,** operculum; **os,** osphradium; **ot,** oral tube; **ov,** pallial oviduct; **pa,** posterior aorta; **pb,** proboscis; **pc,** pericardium; **pg,** pedal gland furrow; **pp,** penis apical papilla; **rs,** radular sac; **rt,** rectum; **rv,** efferent renal vessel; **sd,** salivary duct; **se,** fold of siphonal base; **si,** siphon; **te,** cephalic tentacle; **vd,** vas deferens; **ve,** ventricle; **vs,** blood vessel.

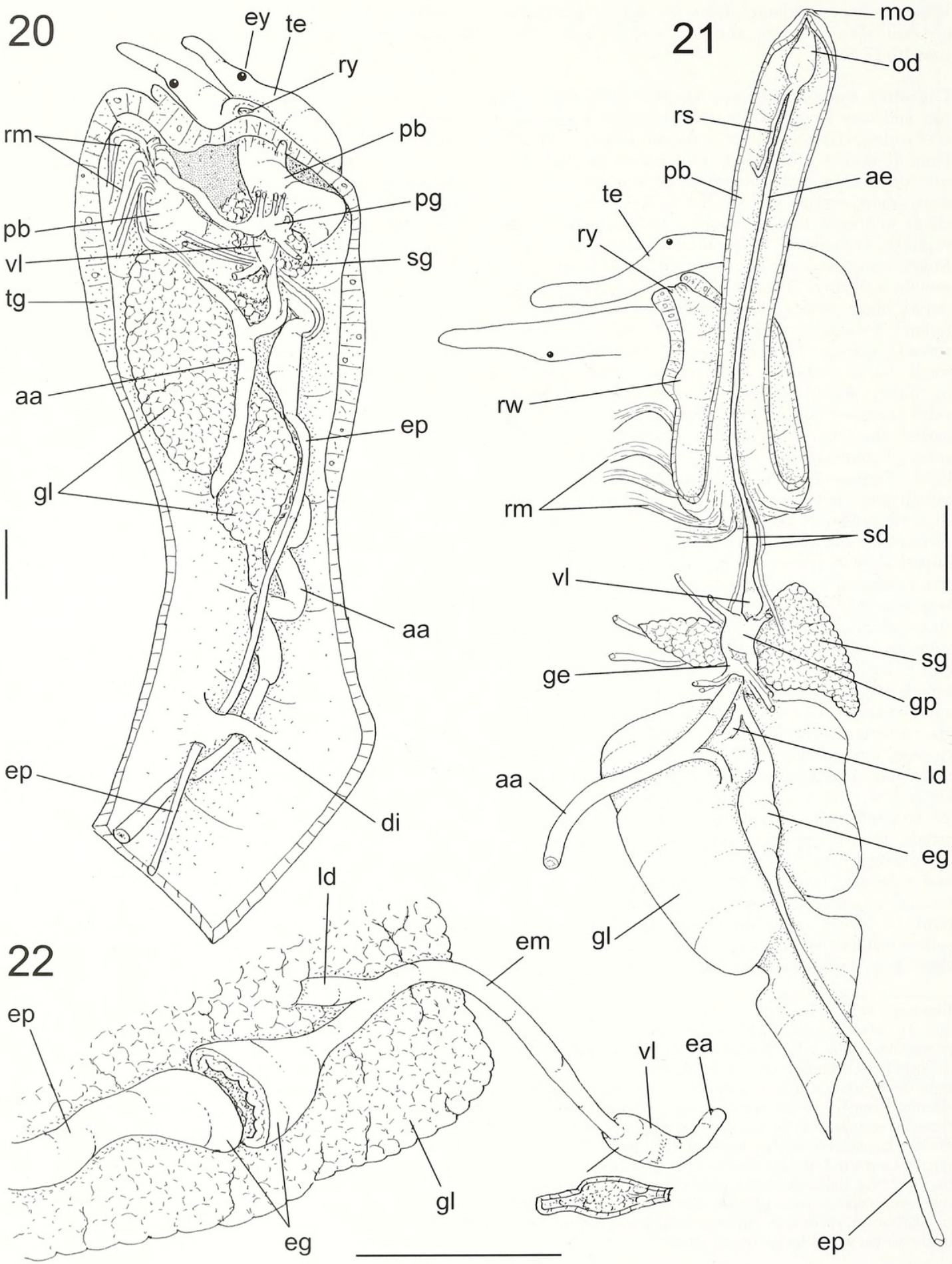
20
ey
te
ry
rm
pb
pg
pb
vl
sg
tg
aa
ep
gl
aa
ep
di
21
mo
od
rs
pb
ae
te
ry
rw
rm
sd
vl
sg
ge
gp
ld
aa
eg
gl
ep
22
ld
em
ep
vl
ea
gl
eg

(Figure 23, **df**). Valve of Leiblein slightly wider than surrounding esophagus, anterior half conical, posterior half rounded (Figure 22). Internally, valve anterior with a tall cylindrical fold, with relatively short cilia directed posteriorly (Figure 22). Remaining portions of valve of Leiblein entirely covered by inner, thick whitish glandular layer. Middle esophagus about same diameter as anterior esophagus (Figure 21); inner surface smooth, simple. Gland of Leiblein occupying ~1/3 of haemocoel volume, broad, flat anteriorly, gradually narrowing posteriorly, becoming very narrow, sharply pointed (Figures 20, 21). Duct of gland of Leiblein broad, situated at some distance from anterior end of gland. Posterior esophagus narrow, equal in length to anterior esophagus (Figures 21, 26), with a broadly expanded glandular region (Figures 21, 22, **eg**) situated beneath gland of Leiblein, posterior to duct of gland of Leiblein (by ~1/10 posterior esophagus length). Glandular lining of this region of posterior esophagus about twice as thick as esophageal wall. Stomach a simple curve (Figure 26), equal in width to esophagus, located about 1/3 whorl posterior to kidney, embedded in digestive gland. Inner surface smooth, simple. Duct to digestive gland single, joining stomach in posterior gastric curve, about equal in diameter to intestine. Intestine as wide as esophagus, nearly straight, running anteriorly along right region of visceral mass, passing through ventral region of renal lobe (Figure 17). Digestive gland, rectum and anus described above.

Male Genital System (Figures 14, 27–29, 36): Visceral vas deferens running from testis along columellar surface of visceral mass to intensely coiled seminal vesicle located on mid-ventral region of last whorl of visceral mass, comprising ~1/4 of mass of adjacent region of visceral mass (Figure 29, **sv**). Vas deferens narrow, simple, straight, running along ventral wall of kidney, exiting into mantle cavity along its middle-posterior edge (Figure 29, **vd**). Pallial vas deferens strongly convoluted for 1/4 of mantle cavity length along right-ventral edge of mantle cavity, connecting to posterior end of prostate gland. Prostate gland ~1/4 of mantle cavity length, ~1/10 its width (Figure 28, **pt**), with glandular, iridescent, walls narrowing anteriorly, lacking clear separation with remaining anterior vas deferens, which crosses to pallial floor at level of anus, winding sigmoidally to base of penis (Figures 14, 27, 36); pallial vas deferens entirely closed (tubular) (Figure 27, **vd**). Penis broadest medially (1/3 penis length), somewhat flattened, occupies ~1/6 mantle cavity volume, curved at base; apical region narrowing abruptly, rounded; apical papilla narrow, ~1/8 of penis length, located within protective apical chamber that occupies ~1/10 of penis volume (Figure 27). Penis duct (~1/6 of penis width) runs along penis axis, strongly coiled at mid-length (Figure 27), narrowing at papilla base, opening at papilla tip.

Female Genital System (Figures 16, 32, 33): Visceral oviduct relatively wide, entering left posterior region of albumen gland (Figure 32). Pallial oviduct massive (Figure 16), (~2/3 length, ~1/3 width of mantle cavity). Albumen gland spherical, flattened, walls thick, white, about ~1/4 pallial oviduct length; lumen broad and flat, continuous with that of capsule gland. Capsule gland long (~2/3 pallial oviduct length), slightly narrower than, and anterior to, albumen gland; walls thick, glandular, pale beige in color; lumen broad and flat (Figure 32). Anterior region of capsule gland with thinner walls, forming vaginal atrium (Figures 32, 33, **vg**). Bursa copulatrix elliptical, ~1/6 pallial oviduct length, situated on ventral, left side of anterior end of pallial oviduct. Bursa walls thick, longitudinally folded. Capsule gland and bursa copulatrix ducts converge anteriorly to form small genital papilla (Figure 33, **fp**), located within small chamber.

Central Nervous System (Figures 20, 21, 30, 31): Nerve ring located in anterior region of haemocoel, at proboscis base (Figures 20, 21). Nerve ring volume approximately 1/20 that of haemocoel. Ganglia highly concentrated and difficult to separate. Cerebral and pleural ganglia paired, totally fused. Pedal ganglia paired, as large as cerebro-pleural ganglia, broadly connected to each other and to remaining main ganglia. Sub-esophageal ganglion close to nerve ring, about half the size of a pedal ganglion. Statocysts not found.

Measurements (in mm): MZSP 63824: ♀1: 64.7 by 33.1; ♂3: 47.4 by 25.8; MZSP 64213 ♀1: 62.1 by 28.4; PRI 9468: 40.0 by 22.3 (Figs. 1–3).

Geographic Distribution: Baja California to Peru.

Habitat: Under rocks, intertidal and subtidal.

Material Examined: W. PANAMA (Gulf Panama): Panamá City, MZSP 10173, 1 shell; Chumical Arerajan, Chumical Bay Playa, 08°53′08.8″ N, 79°38′37.7″ W, MZSP 63824, 1♂, 2♀ (Simone col., 29 Jan. 2006); Venado Island, 08°52′48.6″ N, 79°35′36.9″ W, MZSP 64213, 4♂, 2♀ (Simone col. 30 Jan. 2006), MZSP 77671,

Figures 20–22. *Vitularia salebrosa* anatomy. **20.** Head and haemocoel, ventral view, foot and columellar muscle removed, inner structures as in situ. **21.** Foregut removed, ventral view, some adjacent structures also shown. **22.** Detail of foregut region between valve and gland of Leiblein, ventral view, with detail of valve opened longitudinally, a transversal section artificially done in proximal region of posterior esophagus. Scale bars = 2 mm. Abbreviations: **aa,** anterior aorta; **ae,** anterior esophagus; **di,** diaphragm-like septum; **ea,** anterior esophagus; **eg,** gland of posterior esophagus; **em,** middle esophagus; **ep,** posterior esophagus; **ey,** eye; **ge,** sub-esophageal ganglion; **gl,** gland of Leiblein; **gp,** pedal ganglion; **ld,** duct of gland of Leiblein; **mo,** mouth; **od,** odontophore; **pb,** proboscis; **pg,** pedal gland furrow; **rm,** proboscis retractor muscle; **rs,** radular sac; **rw,** rhynchodeal wall; **ry,** rhynchostome; **sd,** salivary duct; **sg,** salivary gland; **te,** cephalic tentacle; **tg,** integument; **vl,** valve of Leiblein.

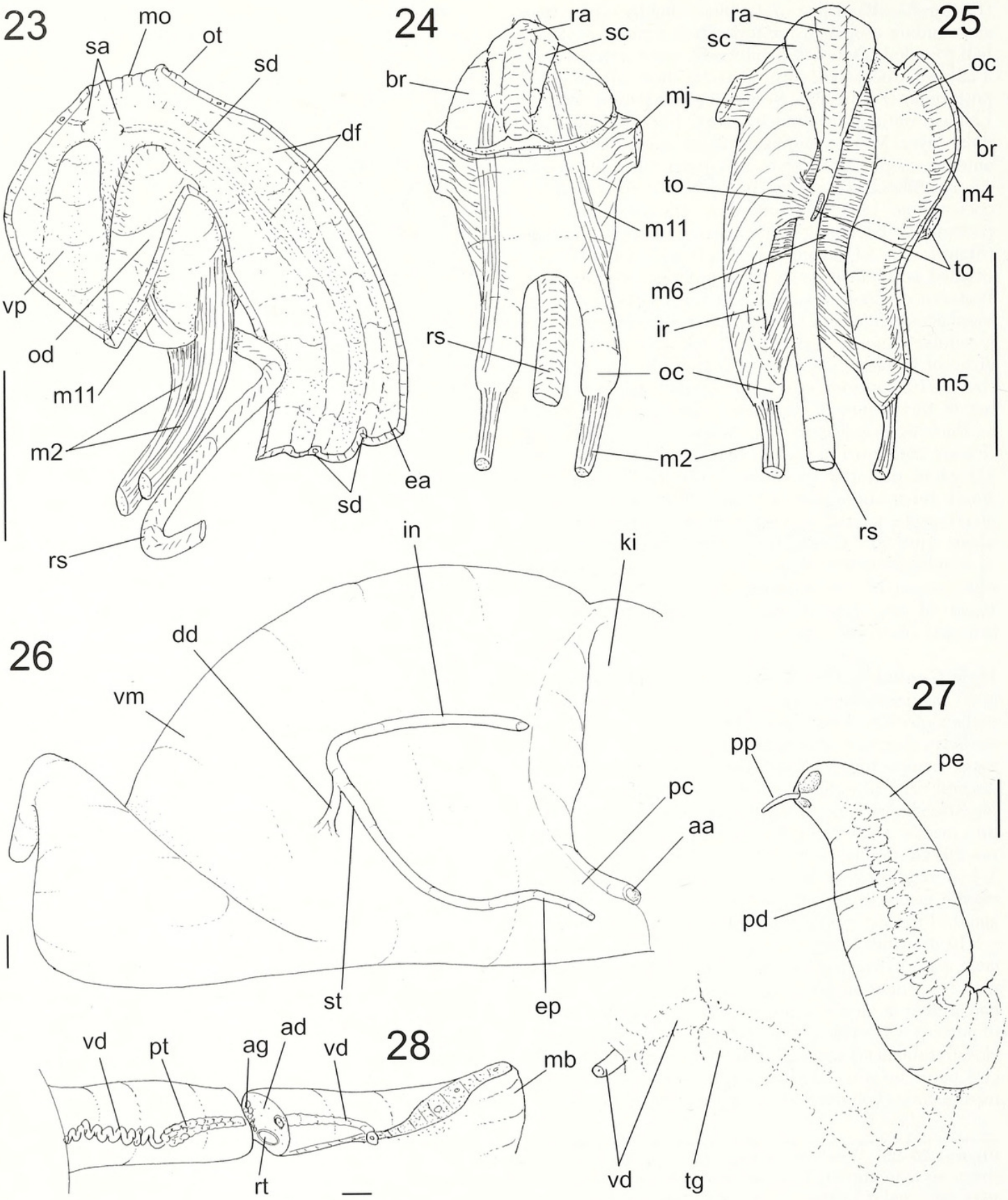
23
mo
ot
sa
sd
df
vp
od
m11
m2
ea
sd
rs
24
ra
sc
br
mj
m11
rs
oc
m2
25
ra
sc
oc
br
to
m4
to
m6
ir
m5
rs
26
in
ki
dd
vm
pc
aa
st
ep
27
pp
pe
pd
28
vd
pt
ag
ad
vd
mb
rt
vd
tg

3♀, 83792, 7 specimens (Simone col. 01/ii/2006), PRI 9468, 2 specimens (Figures 1–3, 6–8). Las Perlas Archipelago, 08°21′27.7″ N, 78°50′28.7″ W, MZSP 78481, 2 specimens (Simone col. 4 Feb. 2006). COSTA RICA: Joce Beach, PRI 9469, 1 specimen. ECUADOR: Manabi; Isla Salango, MZSP 67408, 1 shell, MZSP 69597, 12 shells (Coltro col. Mar. 2003).

DISCUSSION

The anatomy of *Vitularia salebrosa* is comparable to that described for numerous muricids (e.g., Harasewych, 1984; Kool, 1987, 1993a, b; Ball et al., 1997; Tan and Sigurdsson, 1996; Tan, 2003; Simone, 2007), and shares features characteristic of the family, among them a mantle border that closely surrounds the siphon, an accessory boring organ, and an anal papilla. However, several aspects of the morphology of *V. salebrosa* appear to be unique. These include: (1) a tall, septum-like fold at the right base of the siphon (Figure 16, **se**); (2) an elongated proboscis (Figure 21) (muricids normally bear a well-developed, but shorter proboscis); (3) a small and simple buccal mass, particularly the odontophore (Figure 19), with small **m6** and retractor muscle pairs **m5**, and the lack of a muscular connection in the radular sac (Figures 24, 25); (4) a relatively small pair of lateral teeth on the radula (Figures 9–12); (5) a digestive system that is simplified and reduced in diameter (Figures 21, 22, 26), particularly the stomach, which is reduced to a simple, inconspicuous curve that is joined by the duct of the digestive gland; (6) a reduced valve of Leiblein that lacks a transverse furrow, or by-pass, along its length (Figure 22, **vl**); (7) a mid-esophagus that is simple, rather than glandular as in most muricids (Figures 21, 22, **eg**); (8) an anal gland (Figure 32, **ag**) that is unusually elongated; (9) a prostate gland that is relatively small, with a long, convoluted vas deferens in the mantle cavity (Figure 28); (10) a penis with a terminal papilla (common in muricids) that is protected by an unusual terminal chamber. Similarly, the female genital pore is also protected in a small, hollow chamber (Figure 33), while the remainder of the pallial oviduct is normal for the family; and (11) a central nervous system, or nerve ring, that is more concentrated than usual (Figures 30, 31) (normally, the muricid nerve ring is slightly longer dorso-ventrally, with a clearer separation between the pedal ganglia and the remaining ganglia).

This study did not confirm the findings of D'Attilio (1991) and Herbert et al. (2008), who reported that as many as 80–90% of animals studied lacked a radula. All animals dissected in this analysis (n=23) possessed a radula. The different results obtained herein can be interpreted several ways. Herbert et al. (2009) found that ectoparasistic interactions between an individual *Vitularia salebrosa* and a single molluscan host can last many months and possibly as long as a year. They also found that interactions with new oyster prey appear to start at the same time each year. Because *V. salebrosa* requires a radula to initiate the interaction by drilling a feeding hole, it may be that a functioning radula is present sporadically, and perhaps seasonally (see also Herbert et al., 2009). An alternative explanation is that the radula was destroyed by the cleaning process used in past work, which involved dissolving tissues either in concentrated potassium hydroxide, or in a bleach-like solution. It is not clear, however, why this technique works so well for other muricids but would fail consistently for *V. salebrosa*, unless its radula is sometimes non-mineralized. It is also possible that the long proboscis was accidentally amputated by collectors vigorously pulling the feeding animal from its host. Each of these explanations can be easily tested in future work.

Differences in the digestive system between *Vitularia salebrosa* and other muricids, particularly the simplification and reduction in diameter of its gut, are compatible with an ectoparasitic mode of life. On the other hand, as the digestive system is complete in *V. salebrosa*, it is possible to infer that parasitism is not obligatory, and that normal predatory behavior can also occur. The muricid subfamily Coralliophilinae is known to include species that are ectoparasitic on cnidarians, yet there are few parallels between the anatomy of coralliophilines and that of *V. salebrosa*. A striking aspect of the anatomy of *V. salebrosa* is the highly reduced diameter of its digestive tract, although it has retained a fully functional buccal mass and odontophore. In contrast, coralliophilines have suffered severe atrophy of the anterior portion of the digestive system, particularly the buccal mass, including the total loss of the odontophore, radula, and related structures. However, the remaining portions of the digestive system in coralliophines are relatively similar to those of other muricids.

Figures 23–28. *Vitularia salebrosa* anatomy. **23.** Buccal mass, right view, esophagus and ventral region opened longitudinally, way of right salivary duct partially shown, radular sac only partially shown. **24.** Odontophore, ventral view. **25.** Same, ventral view, left structures (right in Figure) partially deflected, superficial layer of tissues removed. **26.** Visceral partially uncoiled showing topology of midgut, ventral view, topology of some portions of reno-pericardial structures also shown. **27.** Penis and adjacent region of head, dorsal view, some penial inner structures artificially shown. **28.** Detail of right region of mantle cavity, male, ventral view, with focus on genital structures, a transverse section through middle region. Scale bars = 1 mm. Abbreviations: **aa,** anterior aorta; **ad,** adrectal sinus; **ag,** anal gland; **br,** subradular membrane; **dd,** duct to digestive gland; **df,** dorsal inner folds of buccal mass; **ea,** anterior esophagus; **ep,** posterior esophagus; **in,** intestine; **ir,** insertion of m4 radular sac; **ki,** kidney chamber; **m1–m11,** buccal mass and odontophore muscles; **mb,** mantle border; **mj,** peri-oral muscles; **mo,** mouth; **oc,** odontophore cartilage; **od,** odontophore; **ot,** oral tube; **pc,** pericardium; **pd,** penis duct; **pe,** penis; **pt,** prostate gland; **ra,** radula; **rs,** radular sac; **rt,** rectum; **sa,** salivary duct aperture; **sc,** subradular cartilage; **sd,** salivary duct; **st,** gastric region; **tg,** integument; **to,** tissue connecting m4 with radular sac; **vd,** vas deferens; **vm,** visceral mass; **vp,** ventral platform of buccal mass.

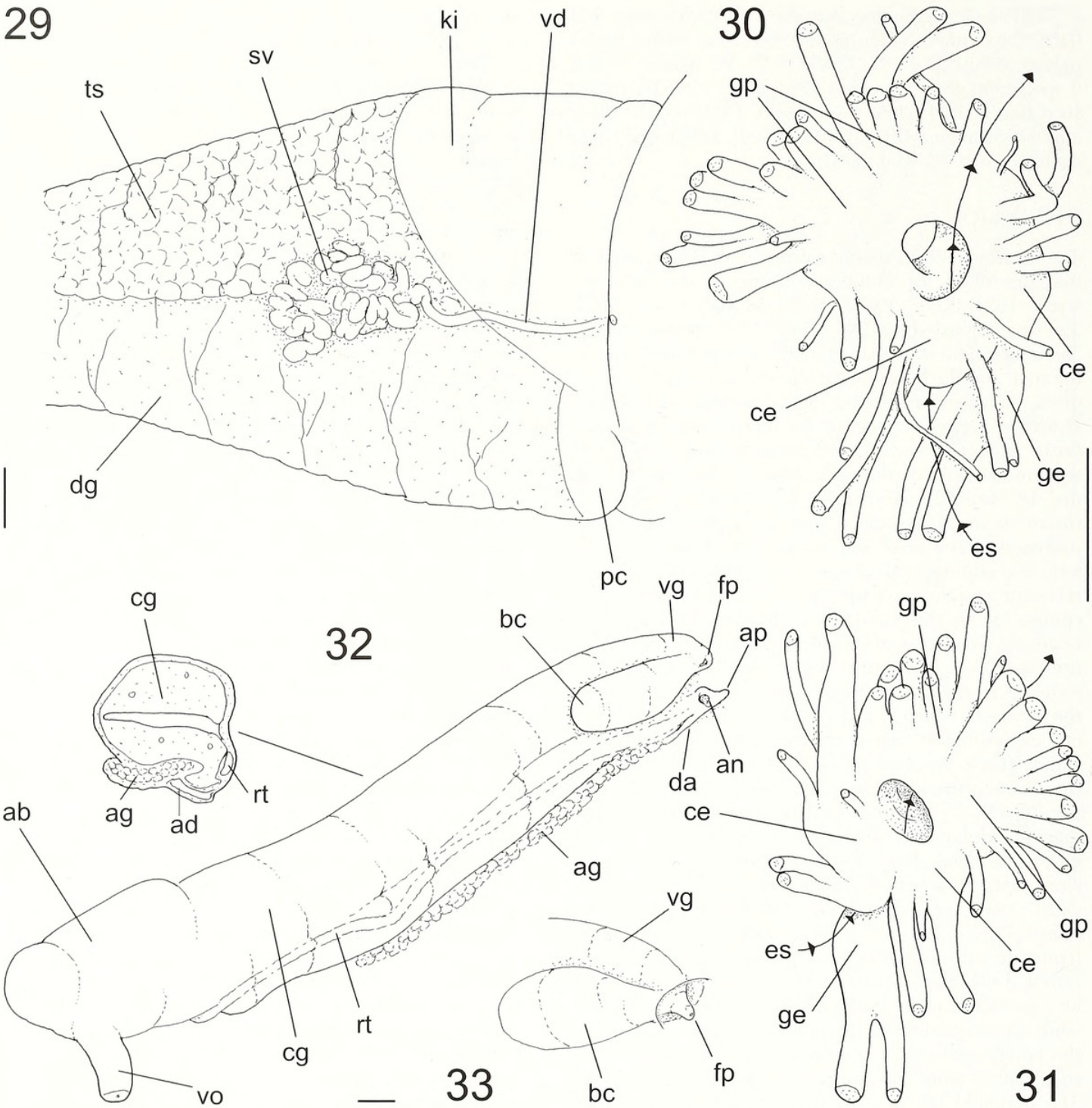

Figures 29–33. *Vitularia salebrosa* anatomy. **29.** Anterior region of visceral mass, male, ventral view. **30.** Nerve ring, ventral view, with indication of esophagus topology (successive arrows). **31.** Same, dorsal view. **32.** Pallial oviduct, ventral view, some adjacent structures also shown, a transversal section of indicated region also revealed. **33**. Detail of anterior region of pallial oviduct, ventral view, with inner terminal genital papilla protruded. Scale bars = 1 mm. Abbreviations: **ab,** albumen gland; **ad,** adrectal sinus; **ag,** anal gland; **an,** anus; **ap,** anal papilla; **bc,** bursa copulatrix; **ce,** cerebro-pleural ganglion; **cg,** capsule gland; **da,** anal gland duct; **es,** esophagus; **fp,** female pore; **ge,** sub-esophageal ganglion; **gp,** pedal ganglion; **ki,** kidney chamber; **rt,** rectum; **sv,** seminal vesicle; **ts,** testis; **vd,** vas deferens; **vg,** vaginal atrium; **vo,** visceral oviduct.

ACKNOWLEDGMENTS

The authors thank the Smithsonian Tropical Research Institute marine lab at NAOS, and the government of Panama for collection permits, and Jerry Harasewych and Ellen Strong for organizing fieldwork during the Neogastropod Evolution Workshop in Panama in January 2006. Emily Vokes and Geerat Vermeij kindly provided shells figured in this study from their research collections.

Funding was provided by a University of South Florida faculty improvement grant to GSH. This study is partially supported by a governmental grant from Fapesp (Fundação de Amparo à Pesquisa do Estado de São Paulo) to the senior author, process # 2004/10793-9.

LITERATURE CITED

Ball, A.D., E.B. Andrews, and J.D. Taylor. 1997. The ontogeny of the pleurembolic proboscis in *Nucella lapillus* (Gastropoda: Muricidae). Journal of Molluscan Studies 63: 87–99.

D'Asaro, C.N. 1970. Egg capsules of some prosobranchs from the Pacific coast of Panama. Veliger 13: 37–43.

D'Asaro, C.N. 1991. Gunnar Thorson's world-wide collection of prosobranch egg capsules: Muricidae. Ophelia 35: 1–101.

D'Attilio, A. 1991. Comments on two ambiguous muricids currently comprising the genus *Vitularia* Swainson, 1840. The Festivus 23: 13–15.

Harasewych, M.G. 1984. Comparative anatomy of four primitive muricacean gastropods: implications for Trophoninae phylogeny. American Malacological Bulletin 3: 11–26.

Herbert, G.S., G.P. Dietl, H. Fortunato, J. Sliko, and L.R.L. Simone. 2009. Ectoparasitism by *Vitularia salebrosa* (Neogastropoda: Muricidae) on molluscan hosts: Evidence from predation traces, isotope sclerochronology, and feeding experiments. The Nautilus 123: 121–136.

Herbert, G.S., D.Merle, and C. S. Gallardo. 2008. A developmental perspective on evolutionary innovation in the radula of the predatory Neogastropod family Muricidae. American Malacological Bulletin 23: 17–32.

Keen, A.M. 1971. Sea shells of tropical West America, second edition. Stanford University Press, Stanford, 1064 pp., 22 pls.

King, P.P. and W.J. Broderip. 1832. Description of Cirrhipeda, Conchifera and Mollusca... the southern coasts of South America. Zoological Journal 5(19): 332–349.

Kool, S.P. 1987. Significance of radular characters in reconstruction of thaidid phylogeny (Neogastropoda: Muricacea). The Nautilus 101: 117–132.

Kool, S.P. 1993a. Phylogenetic analysis of the Rapaninae (Neogastropoda: Muricidae). Malacologia 35: 155–259.

Kool, S.P. 1993b. The systematic position of the genus *Nucella* (Prosobranchia: Muricidae: Ocenebrinae). The Nautilus 107: 43–57.

Merle, D. 2001. The spiral cords and the internal denticles of the outer lip of the Muricidae: Terminology and methodological comments. Novapex 2: 69–91.

Merle D. 2005. The spiral cords of the Muricidae (Mollusca: Gastropoda): importance of ontogenetic and topological correspondences for delineating structural homologies. Lethaia 38: 367–379.

Paredes, C., F. Cardoso, and J. Tarazona. 2004. Distribución temporal de moluscos y crustáceos tropicales en la Provincia Peruana y su relación con los eventos El Niño. Revista Peruana de Biología 11: 213–218.

Radwin, G.E. and A. D'Attilio. 1976. Murex shells of the world. Stanford University Press. Stanford, California, 284 pp.

Ramírez, R., C. Paredes, and J. Arenas. 2003. Moluscos del Perú. Revista de Biologia Tropical, Suppl. 3: 225–284.

Simone, L.R.L. 2007. Accounts on the phylogeny of the Muricidae (Caenogastropoda) based on comparative morphology of some representatives. Abstracts, World Congress of Malacology, 2007, Antwerp, Belgium, 15–20 July 2007. Unitas Malacologica, Antwerp, p. 206.

Tan, K.S. 2003. Phylogenetic analysis and taxonomy of some southern Australian and New Zealand Muricidae (Mollusca: Neogastropoda). Journal of Natural History 37: 911–1028.

Tan, K.S. and J.B. Sigurdsson. 1996. Two new species of *Thais* (Mollusca: Neogastropoda: Muricidae) from peninsular Malaysia and Singapore, with notes on *T. tissoti* (Petit, 1852) and *T. blanfordi* (Melvill, 1893) from Bombay, India. Raffles Bulletin of Zoology 44: 77–107.

Vokes, E.H. 1977. A second western Atlantic species of *Vitularia* (Mollusca: Gastropoda). Tulane Studies in Geology and Paleontology 13: 192–195.

Vokes, E.H. 1986. The short happy life of *Vitularia linguabison*. Conchologists of America Bulletin 14: 19–22.